Hadamard-Transform k-t PCA for Cine 3D Velocity Vector Field Mapping of Carotid Flow

V. Knobloch[1], D. Giese[1], P. Boesiger[1], and S. Kozerke[1]

[1]Institute for Biomedical Engineering, Swiss Federal Insitute of Technology and University Zurich, Zurich, Zurich, Switzerland

Introduction

Secondary flow patterns in the carotid bifurcation have been found to promote distinct wall shear stress configurations [1]. To study these effects, Computational Fluid Dynamics (CFD) has been utilized with vessel geometries derived from anatomical MR data [2]. Despite the success of CFD methods providing results at very high resolutions, there is a desire to derive flow patterns directly from phase-contrast MR measurements with immediate visualization of the results [3]. Cine 3D phase-contrast MR permits acquisition of time-resolved velocity vector fields but requires very long measurement times if high spatiotemporal resolutions are required. Parallel imaging methods have been used to shorten the long scan times but net scan reduction factors used in practical situations remain limited. Methods exploiting spatiotemporal correlations have attracted much attention [4,5] and it has been shown recently that k-t PCA (Principle Component Analysis) [6] permits acceleration up to a net factor 10 without compromising the accuracy of single-directional flow quantification. The objective of the present work was to extend k-t PCA to time-resolved 3D vector field mapping using the Hadamard transform as a sparsifyer. Using phantom and in-vivo data the accuracy of the method was assessed for different reduction factors relative to data from fully sampled measurements.

Theory

In k-t PCA reconstruction, the undersampled image information P(x,f) is split into a set of spatially invariant basis functions B(i,f) and a set of temporally independent weighting coefficients W(x,i):

$$P(x, f_m) = \sum_{i=1}^{n} W(x,i)B(i, f_m)$$

where B is derived from the fully sampled training profiles and n denotes the number of basis functions being used. For image reconstruction the weighting coefficients are calculated according to a least squares solution:

$$w_x = M_x^2 E^H (EM_x^2 E^H + \lambda I)^+ P_{alias,x}$$

where M^2 is the signal covariance matrix, E the signal encoding matrix, I the identity matrix, and λ a regularization parameter. Using the Hadamard matrix H the signals P and P_{alias} are transformed into a sparse representation according to:

$$\widetilde{P}^T = P^T(x, f, s)H(s)$$

where s counts the number velocity encoding segments (Figure 1).

Figure 1: Magnitude images of the four velocity encoding segments before (top row) and after (bottom row) Hadamard transformation.

Methods

For phantom experiments pulsatile fluid flow was generated and pumped through an artificial bifurcation. Cine 3D phase-contrast data were acquired using a referenced four point acquisition scheme on a 3T Philips Achieva system (Philips Healthcare, Best, The Netherlands). An 8-channel head coil was used for signal reception. Imaging parameters were: voxel size: $1.4 \times 1.1 \times 1.4mm^3$, TR/TE: 6/2.9ms, venc (FH/RL/AP): 100, 60, 60cm/s.

In-vivo experiments were conducted in healthy volunteers using a 2-channel surface coil for signal reception. Imaging parameters were: voxel size: $1.2 \times 1.5 \times 1.5mm^3$, TR/TE: 7.1/3.2ms, venc (FH/RL/AP): 120, 50, 50cm/s.

Fully sampled data were decimated by factors of R=2, 6, 8 and 10 using optimal undersampling patterns [7] with 11 fully sampled training profiles in y- and 7 in z-direction resulting in net accelerations of 1.8, 5, 6.1 and 7.7, respectively. Data were analyzed using GTFlow (GyroTools, Zurich, Switzerland).

Results

The error in component flow as a function of nominal undersampling factors is plotted in Figure 2. In feet-head (FH) and antero-posterior (AP) directions the error remains below 4% for all undersampling factors tested.. Figure 3 demonstrates pathline visualization on phantom and in-vivo images reconstructed from 6- and 10-fold undersampled data. At 10-fold undersampling the tracking path length is reduced in-vivo indicating the limits of data undersampling.
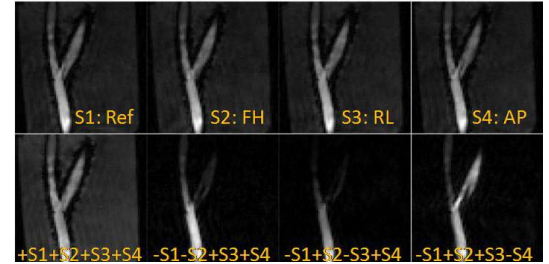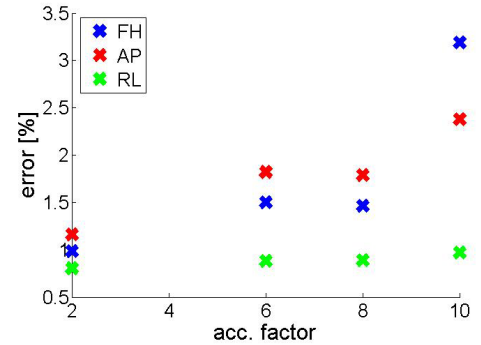
Figure 2: Error in component flow in the common carotid artery as a function of the nominal reduction factor for the three velocity encoding directions (FH, RL, AP).
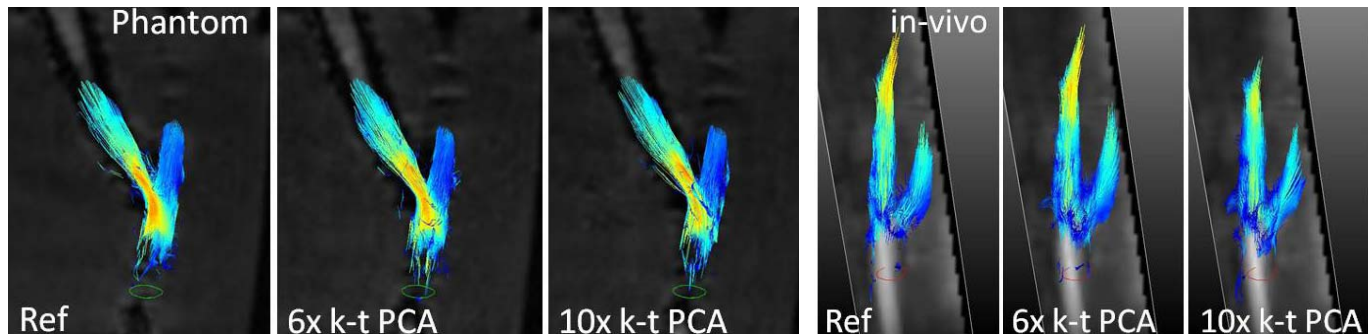
Figure 3: Pathline visualization of 3D velocity vector fields in the bifurcation phantom and in-vivo measurement of the carotid bifurcation.

Discussion

It has been demonstrated that k-t PCA provides faithful representation of velocity vector fields up to very high net reduction factors rendering the method very promising for accelerating 3D cine phase-contrast velocity mapping. Further studies are warranted to validate the approach in patients.

References

[1] Milner JS. et al. J Vasc Surg, 1998; 27:143-56
[2] Steinman DA. et al. MRM, 2002; 47:149-159
[3] Harloff A. et al. MRM, 2009; 61:65-74
[4] Tsao J. et al. MRM, 2003(50):1031-1042
[5] Jung B. et al. JMRI, 2008(28):1226-32
[6] Pedersen H. et al. MRM, 2009; 62:707-716
[7] Tsao J. et al. MRM, 2005(53): 1372-82